



Article

N-Glycosylation as a Key Requirement for the Positive Interaction of Integrin and uPAR in Glioblastoma

Gretel Magalí Ferreira ¹, Hector Adrian Cuello ^{1,2,3}, Aylen Camila Nogueira ^{1,4,5}, Jeremias Omar Castillo ¹, Selene Rojo ¹, Cynthia Antonella Gulino ¹, Valeria Inés Segatori ^{1,5} and Mariano Rolando Gabri ^{1,5,*}

¹ Centro de Oncología Molecular y Traslacional, Universidad Nacional de Quilmes, Bernal B1876BXD, Argentina; maguiferreira2@gmail.com (G.M.F.); hectorcuello@live.com.ar (H.A.C.); aylen.nogueira@gmail.com (A.C.N.); jerecastillo13@gmail.com (J.O.C.); selenerojo25@gmail.com (S.R.); cynthia.gulino@gmail.com (C.A.G.); valeriasegatori@gmail.com (V.I.S.)

² Department of Cellular and Molecular Medicine, University of California San Diego, California, CA 92093, USA

³ Glycobiology Research and Training Center, University of California San Diego, California, CA 92093, USA

⁴ Laboratorio de Glicomedicina, Instituto de Biología y Medicina Experimental (IBYME), Buenos Aires C1428, Argentina

⁵ Consejo Nacional de Investigaciones Científicas y Técnicas (CONICET), Buenos Aires C1425FQB, Argentina

* Correspondence: mrgabri@unq.com.ar

Abstract: Integrin αV (I αV) and the urokinase-type plasminogen activator receptor (uPAR) are key mediators of tumor malignancy in Glioblastoma. This study aims to characterize I αV /uPAR interaction in GBM and investigate the role played by glycans in this scenario. Protein expression and interaction were confirmed via confocal microscopy and co-immunoprecipitation. The role of N-glycosylation was evaluated using Swainsonine (SW) and PNGase F. I αV glycoproteomic analysis was performed by mass spectrometry. Sialic acids and glycan structures in I αV /uPAR interaction were tested using neuraminidase A (NeuA) and lectin interference assays, respectively. Protein expression and their interaction were detected in GBM cells, but not in low-grade glioma cells, even in cells transfected to overexpress uPAR. SW, PNGase, and NeuA treatments significantly reduced I αV /uPAR interaction. Also, lectin interference assays indicated that $\beta 1$ -6 branched glycans play a crucial role in this interaction. Analysis of the I αV glycosylation profile revealed the presence of complex and hybrid N-glycans in GBM, while only oligomannose N-glycans were identified in low-grade glioma. N-glycosylation inhibition and sialic acid removal reduced AKT phosphorylation. Our findings demonstrate, for the first time, the interaction between I αV and uPAR in GBM cells, highlighting the essential role of N-glycosylation, particularly $\beta 1$ -6 branched glycans and sialic acids.

Keywords: I αV ; uPAR; N-glycosylation; sialic acid



Academic Editor: Stergios Boussios

Received: 21 April 2025

Revised: 23 May 2025

Accepted: 30 May 2025

Published: 31 May 2025

Citation: Ferreira, G.M.; Cuello, H.A.; Nogueira, A.C.; Castillo, J.O.; Rojo, S.; Gulino, C.A.; Segatori, V.I.; Gabri, M.R. N-Glycosylation as a Key Requirement for the Positive Interaction of Integrin and uPAR in Glioblastoma. *Int. J. Mol. Sci.* **2025**, *26*, 5310. <https://doi.org/10.3390/ijms26115310>

Copyright: © 2025 by the authors. Licensee MDPI, Basel, Switzerland. This article is an open access article distributed under the terms and conditions of the Creative Commons Attribution (CC BY) license (<https://creativecommons.org/licenses/by/4.0/>).

1. Introduction

Glioblastoma multiforme (GBM) is the most common and aggressive primary brain tumor affecting adults and accounts for 45.6% of all malignant primary brain tumors. The age-adjusted annual incidence of GBM increases with age, from 0.15 per 100,000 in children to a peak of 15.03 per 100,000 in patients aged 75–84 years. Regrettably, current therapies do not yield satisfactory outcomes. On average, GBM patients survive for only 12–18 months. However, 25% of these individuals live beyond a year, and 5% survive for more than five years [1]. A better understanding of the biology of GBM is crucial for unraveling its complexities and discovering new therapeutic targets.

Integrins are heterodimeric proteins composed of both the α and β subunits. In vertebrates, 18 different α and 8 different β subunits have been described, allowing the assembly and expression of 24 distinct heterodimers [2]. Integrin–ligand pairings can be categorized into four primary classes, determined by the type of molecular interaction involved. In particular, all α V-containing integrins together with two β 1 integrins, as well as α IIb β 3, have been described as RGD receptors since they recognize short peptide sequences present in several extracellular matrix (ECM) proteins, such as vitronectin, fibronectin, and fibrinogen [3]. The role of RGD receptor integrins lies primarily in the regulation of cell behavior in response to the extracellular microenvironment. Altered integrin signaling is known to promote the invasive behavior of tumor cells, influence the tumor microenvironment to facilitate angiogenesis [4], participate in the interaction between the ECM and tumor cells [5,6], promote cancer immune escape [7,8], regulate stem cell function [9,10], and participate in the organ-specific targeting of metastatic cancer cells [11]. The expression of the α V β 3 and α V β 5 heterodimer has been widely described to be associated with malignant features of GBM [12–15]. α V β 3 was the first integrin to be abundantly detected in high-grade brain tumors [16], with almost 60% positivity reported in GBM samples [17]. Extensive research has underscored its role in sustaining GBM's high proliferation rate, enhancing migratory and invasive capabilities, and promoting angiogenesis [18,19]. Furthermore, integrin participation in tumor radio- and chemo-resistance has been reported [20,21].

The association between integrin and urokinase-type plasminogen activator receptor (uPAR) has been described in several tissues and in tumors, in which it modulates signaling and cell behavior. uPAR is a glycosylated single-chain protein GPI-anchored with a molecular weight ranging from 50 kDa to 60 kDa. It exerts control over the plasminogen activation system, an extracellular proteolytic cascade, through its interaction with the serine protease urokinase-type plasminogen activator (uPA) and its inactive zymogen form, pro-uPA [22]. In addition to regulating extracellular plasmin activity, uPAR is a signaling receptor. It has been reported that signaling through uPAR activates the Ras-mitogen-activated protein kinase (MAPK) pathway, the Tyr kinase focal adhesion kinase (FAK), and the Rho family small GTPase Rac. Furthermore, FAK signaling can activate PI3K-Akt/PKB [23–26], which participates in the modulation of cell motility, invasion, proliferation, and survival. Since uPAR lacks a transmembrane domain, it requires cooperation with transmembrane receptors to drive intracellular signaling. The expression of uPAR has been highlighted in several cancers as a key factor in malignant behavior, and uPAR has been proposed as a poor prognostic marker [27]. In particular, the overexpression of uPAR in GBM is involved in epithelial–mesenchymal transition, and its association with poor prognosis has been reported [28,29]. Although several membrane proteins have been identified as possible co-receptors of uPAR, substantial evidence points to integrins as the main and most significant co-receptors of uPAR signaling [30,31]. In this regard, numerous pieces of evidence confirm that the interaction between integrins and uPAR is established mainly between the β -propeller region of the integrin α chain and uPAR domain III [32,33].

Even though both are glycosylated proteins, very little evidence provides information on the involvement of glycans in this interaction [34]. Despite significant advances in understanding the role of glycans in several types of tumors, the impact of glycosylation and the potential of glycans as therapeutic targets still merit further investigation [35]. Aberrant glycosylation involves changes in the glycosylation patterns of normal cell progenitors and occurs alongside the multistep process of malignant transformation [36]. These altered glycosylation profiles are linked to cellular characteristics that facilitate tumor progression, including adhesion to the ECM, migration, invasion, inhibition of apoptosis, host immunoregulation, and resistance to chemotherapy [37].

In this study, we demonstrated the interaction between integrin αV ($I\alpha V$) and uPAR in human GBM cells and identified a differential pattern of glycans in the low-grade counterpart. In addition, we present compelling evidence of the significant role played by N-glycosylation in this interaction.

2. Results

To begin to explore the interaction between uPAR and $I\alpha V$, we first examined the expression of glycoproteins in A172 and LN229 human GBM cell lines and in SW1088 human glioma of low grade by WB. Our results showed that these proteins are expressed in both GBM cell lines, although in SW1088 uPAR expression could not be detected (Figure 1A). To evaluate the interaction between these two glycoproteins, we first performed CM image analysis. Pearson's coefficient analysis revealed a high co-localization rate of these two glycoproteins in both GBM cell lines (Figure 1B). In the same line, Co-IP confirmed this interaction in both cell lines when IP was performed on $I\alpha V$ or uPAR (Figure 1C). Since uPAR was not detected in the SW1088 cell line, PLAUR gene transfection was conducted to induce uPAR expression in these cells, which were subsequently designated as uSW1088 (Figure 1A). Notably, although uPAR expression was confirmed in uSW1088 cells, no molecular interaction between this protein and $I\alpha V$ was detected (Figure 1B,C).

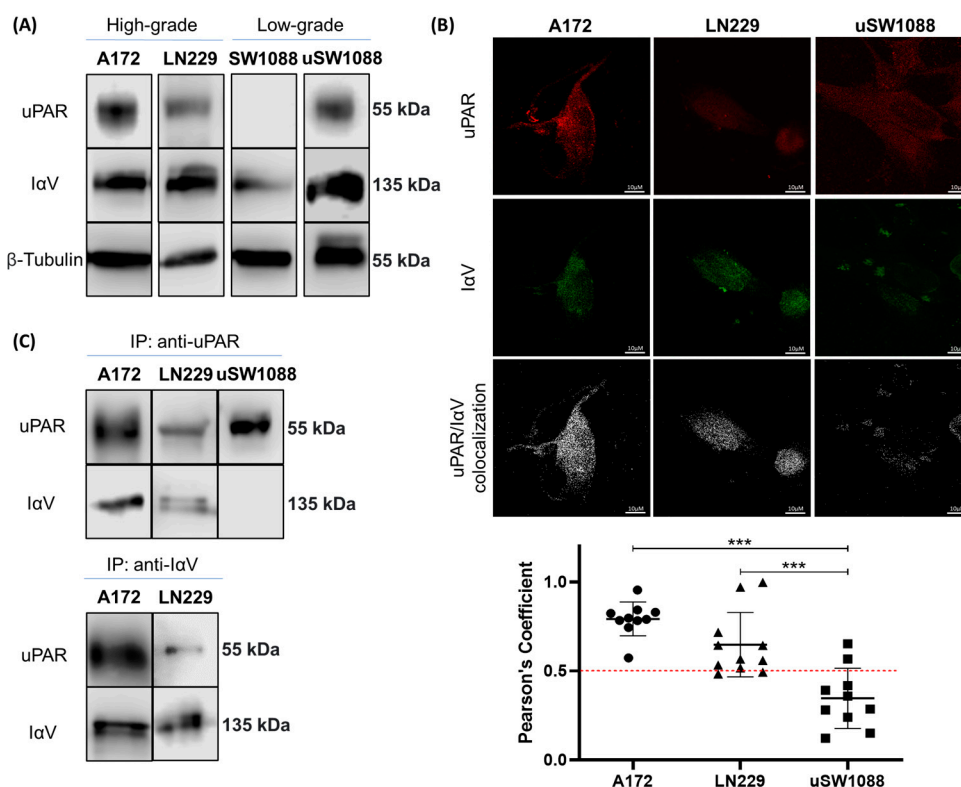


Figure 1. Interaction between $I\alpha V$ and uPAR in human glioma cell lines. (A) Representative WB analysis of $I\alpha V$, uPAR, and β -tubulin expression in equal aliquots of whole-cell lysates from the A172, LN229, SW1088, and uSW1088 cell lines. (B) Protein co-localization analysis of CM from the A172, LN229, and uSW1088 cell lines. uPAR and $I\alpha V$ are shown in red and green, respectively, while co-localization is shown in white. Pearson's coefficient analysis of a representative experiment of three independent datasets showing the means \pm S.D. obtained from single cells of ten fields. (C) Evaluation of protein interactions through co-IP followed by WB. (***) $p < 0.001$, ANOVA followed by Tukey's multiple comparisons test).

Given that both uPAR and $I\alpha V$ are glycosylated proteins with multiple N-glycosylation sites [38–41], we questioned to what extent this type of glycosylation is involved in their

interaction. SW specifically inhibits alpha-mannosidase II, an essential enzyme for the maturation of N-linked glycoproteins [42–44]. PNGase is an enzyme that cleaves N-linked glycans from glycoproteins by targeting the glycosidic bond between the asparagine residue of the protein and the first N-acetylglucosamine of the glycan [42,43,45]. Figure 2A shows that both treatments were able to reduce N-glycosylation in the treated cells, as evidenced by the low staining observed by incubation with PHA-L. As shown by CM analysis, Pearson's co-localization coefficient was nearly 50% lower for control cells than for SW- or PNGase-treated cells (Figure 2B). Similarly, when Co-IP assays were performed, no I α V/uPAR interaction was detected by WB in the treated cells (Figure 2C).

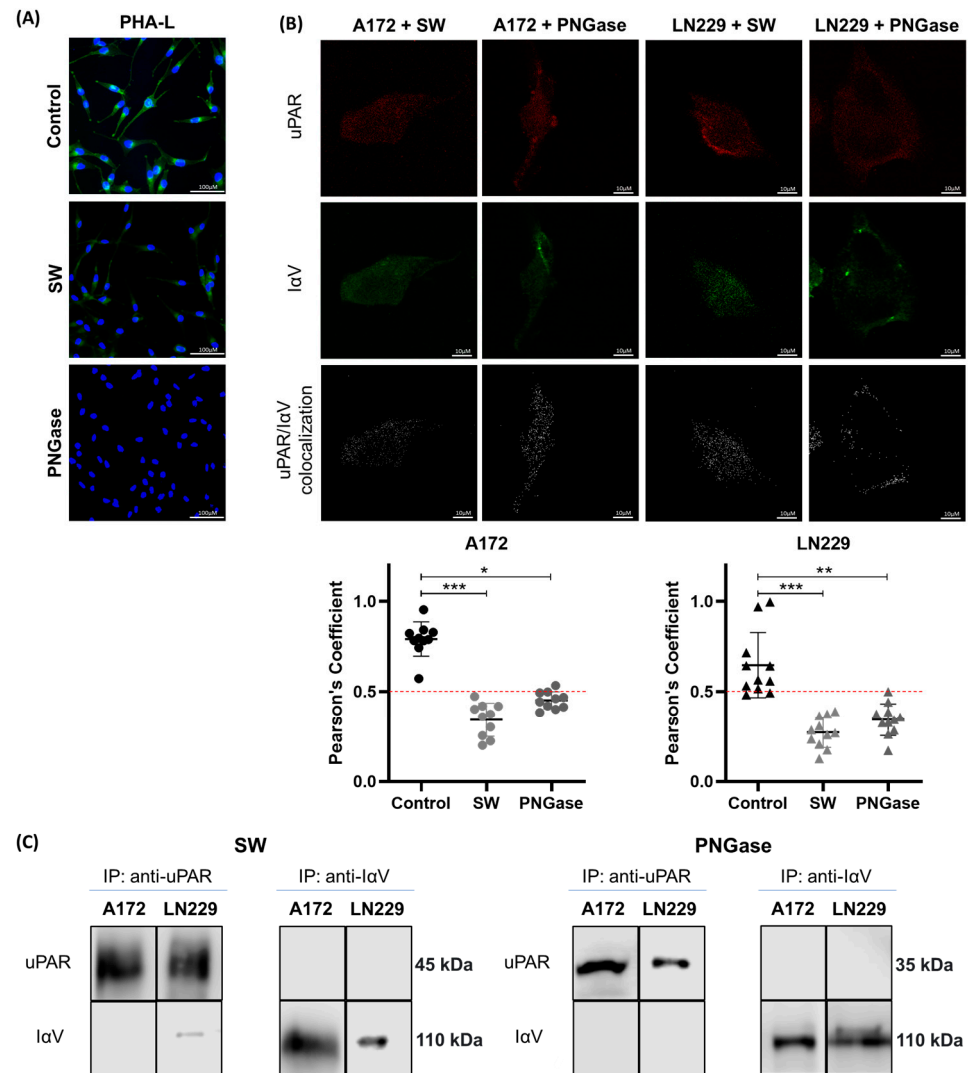


Figure 2. Effect of N-glycosylation inhibition on the interaction between I α V and uPAR in the A172 and LN229 cell lines. (A) PHA-L lectin binding after SW or PNGase treatment through immunofluorescence from the A172 cell line. PHA-L lectin and DAPI staining are shown in green and blue, respectively. (B) Protein co-localization analysis of CM after SW or PNGase treatments. uPAR and I α V are shown in red and green, respectively, while co-localization is shown in white. Pearson's coefficient analysis of a representative experiment of three independent datasets showing the means \pm S.D. obtained from single cells of ten fields (* $p < 0.05$, ** $p < 0.01$, *** $p < 0.001$, Mann–Whitney). (C) Co-IP of proteins followed by WB after treatment with SW or PNGase.

The amino acid sequence of I α V, stored in the UniProtKB/Swiss-Prot repository, predicted the existence of 12 potential N-glycosylation sites (UniProt ID: P06756). Upon MS analysis of the I α V obtained from the GBM cell line LN229, 6 of these 12 sites were found to

be N-glycosylated (Table S1). To map and characterize all the potential glycan structures of each specific glycosite, the m/z values obtained from the MS-based glycoproteomic strategy were used. The main glycan structures for each position are depicted in Figure 3A. The results showed that Asn704 contains only complex/hybrid N-glycans, while only oligomannose N-glycans are present at Asn945. In addition, at Asn74, Asn554, and Asn874, mostly complex/hybrid N-glycans were present, with a decreased abundance of core (Man α 1-3(Man α 1-6)Man β 1-4GlcNAc β 1-4GlcNAc β 1-Asn-X-Ser/Thr) or oligomannose structures. On the other hand, at Asn615, a higher percentage of oligomannose-type N-glycans was detected. With respect to the presence of sialic acid, only the glycan at Asn945 had no sialic acid present, whereas the glycan containing N-glycolylneuraminic acid (NeuGc), N-acetylneuraminic acid (NeuAc), or both were observed at all the other glycosites. The detection of NeuGc—a non-natural sialic acid in human cells—can be explained by the presence of this carbohydrate in the culture media, since its active incorporation by cancer cells from its microenvironment has been reported [46,47]. Conversely, the analysis of I α V glycosylation in the low-grade SW1088 cell line revealed glycan structures at only two glycosylation sites, Asn74 and Asn874, where only oligomannose structures were present. No sialic acid was detected in the SW1088 cell line. The relative expression levels given the microheterogeneity of the N-glycans associated with each glycosite of the protein are shown in Figure 3B.

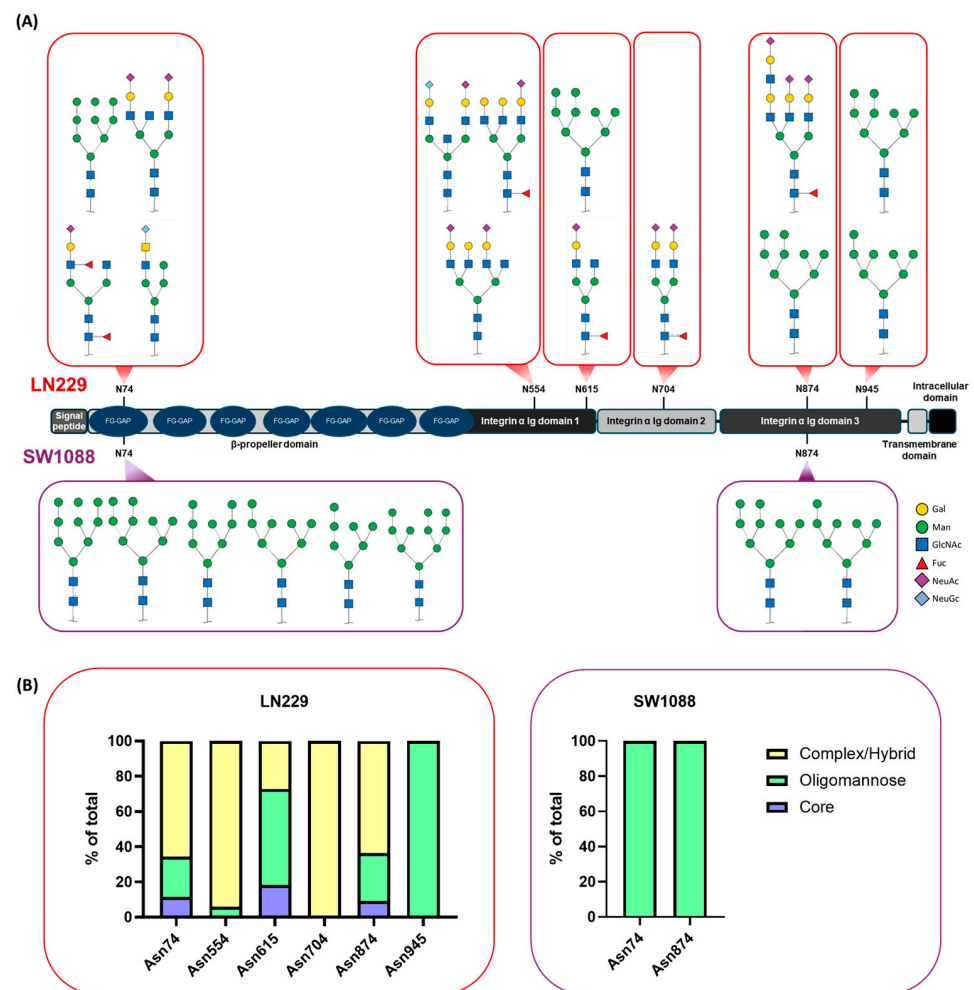


Figure 3. Analysis of the N-glycans of I α V from low-grade tumors and GBM cell lines. (A) Representation of the microheterogeneity of N-glycans on the I α V protein in the LN229 and SW1088 cell lines. (B) Relative abundance of core, oligomannose, and complex/hybrid N-glycans at each I α V position in LN229 or SW1088 cells.

To determine the participation of sialic acids in the interaction between I α V and uPAR, cultured cells were treated with NeuA, an enzyme that removes the terminal sialic acids of glycan structures. As shown in Figure 4, NeuA treatment decreased I α V/uPAR colocalization, as determined by CM and Co-IP assays in both GBM cell lines.

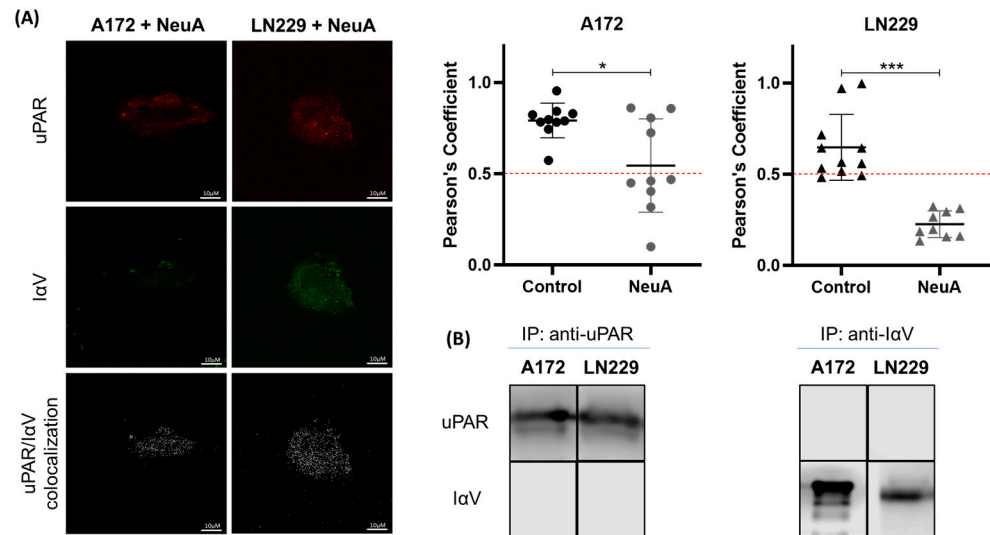


Figure 4. Effect of sialylation on the interaction between I α V and uPAR. (A) Representative protein co-localization analysis of CM after treatment with NeuA. uPAR and I α V are shown in red and green, respectively, while co-localization is shown in white. Pearson's coefficient analysis of a representative experiment of three independent datasets showing the means \pm S.D.s obtained from single cells of ten fields (* $p < 0.05$, *** $p < 0.001$). Mann–Whitney). (B) Co-IP of proteins followed by WB analysis after treatment with NeuA.

To further our analysis, the interference of glycan-mediated protein interactions was evaluated using lectins. The PHA-L lectin mainly binds to β 1-6 branched N-glycans, which were detected at the N74, N554, and N874 glycosylation sites of I α V in the GBM cell line. ConA recognizes oligomannose-type N-glycans that are detected at the N945 glycosylation site in both glioma and GBM cell lines and at the N74, N554, N615, and N874 glycosylation sites in the I α V from the GBM cell line. As expected from the glycosylation profile of GBM cells, incubation with PHA-L lectin strongly inhibited the interaction between I α V and uPAR. However, no effect was observed after ConA incubation (Figure 5), indicating the participation of β 1-6 branched N-glycans in the I α V/uPAR interaction.

Finally, to assess the impact of glycans on I α V/uPAR-associated signaling pathways, AKT phosphorylation was evaluated in response to SW and NeuA. Both treatments resulted in decreased AKT phosphorylation in the LN229 and A172 cell lines. Interestingly, the upregulation of uPAR expression in these cell lines by transfection of the PLAUR gene resulted in increased AKT phosphorylation in the cells named uLN229 and uA172, suggesting the active involvement of uPAR in this signaling pathway. Similarly, SW or NeuA treatment strongly inhibited AKT phosphorylation in these cells (Figure 6).

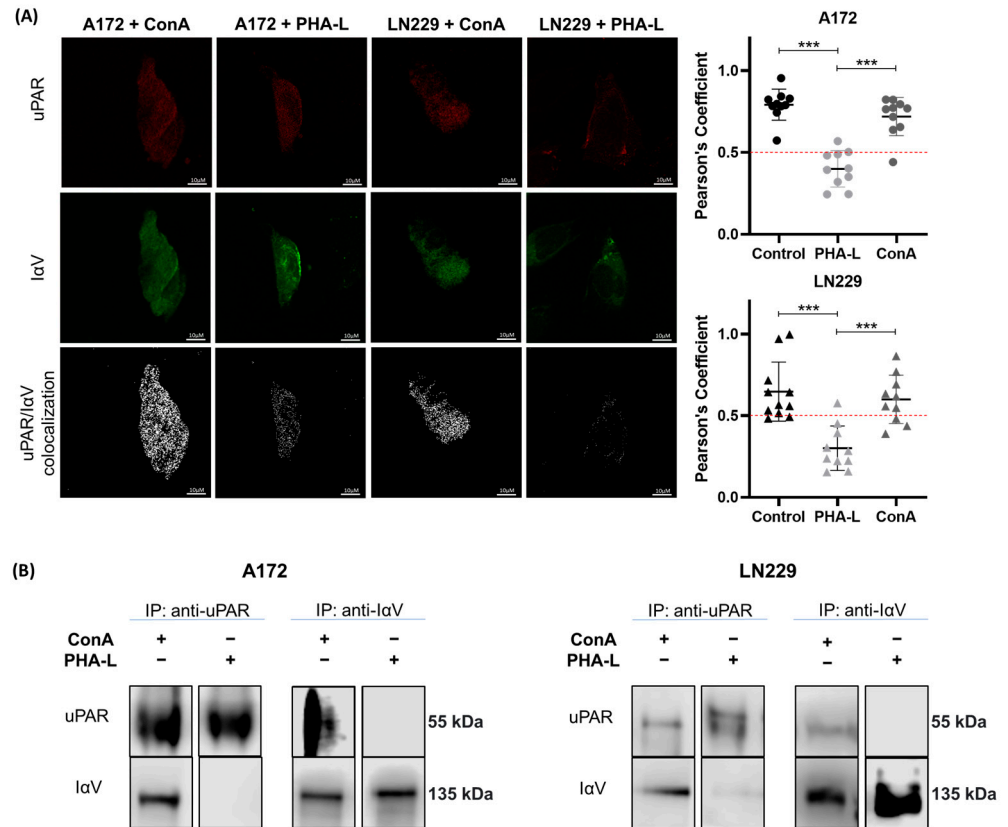


Figure 5. Evaluation of the effect of lectin interference on the interaction between IαV and uPAR. (A) Protein co-localization by CM after incubation with ConA or PHA-L. uPAR and IαV are shown in red and green, respectively, while co-localization is shown in white. Pearson's coefficient analysis of a representative experiment of three independent datasets showing the means ± S.D obtained from single cells of ten fields (***) $p < 0.001$, ANOVA followed by Tukey's multiple comparisons test). (B) Co-IP of proteins and WB after incubation with ConA or PHA-L.

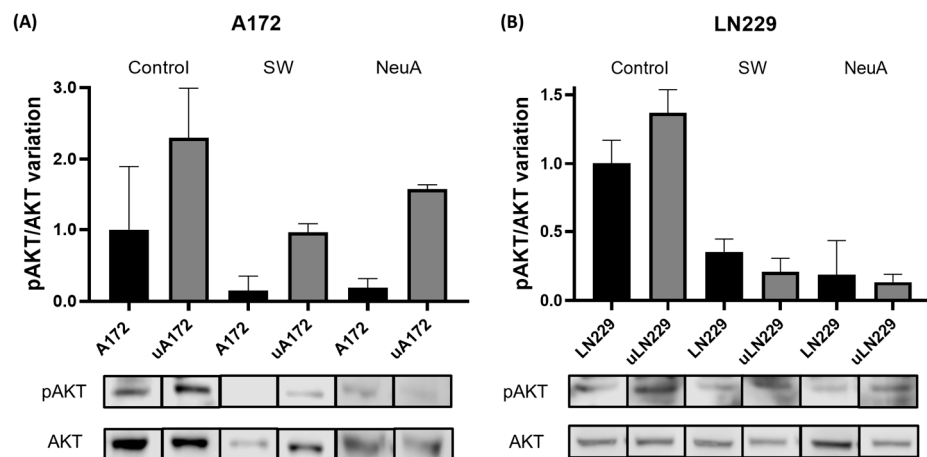


Figure 6. Effect of glycosylation inhibition on AKT pathway activation. Western blot showing pAKT and AKT expression and the pAKT/AKT variation after SW or NeuA treatment in (A) the A172 and uA172 cell lines or (B) the LN229 and uLN229 cell lines. The data are shown as a percentage of the control (WT).

3. Discussion

The interaction between uPAR and integrins is highly relevant in the progression of many types of cancer, and these proteins are key players in processes such as cell migration, invasion and metastasis. uPAR, a glycosylphosphatidylinositol-anchored cell

surface receptor, binds to uPA, activating proteolytic cascades that degrade the ECM and facilitating tumor cell invasion. In parallel, uPAR can trigger intracellular signaling, thereby modulating physiological processes such as wound healing, immune responses and stem cell mobilization, as well as pathological events, including inflammation and tumor progression [48,49]. Integrins and integrin-dependent processes play crucial roles in nearly every phase of cancer progression by actively participating in signaling pathways that promote cell survival, proliferation, and metastasis [50–52]. Both cell membrane receptors have been identified as key contributors to GBM malignancy.

Interactions between integrin and uPAR have been shown in several other tumors. For instance, in gastrointestinal cancers, the interaction between $\alpha V\beta 6$ and uPAR is implicated in the regulation of downstream signaling following uPA binding [30,32] and in the induction of MMP9 secretion, thus facilitating the degradation of multiple ECM components [53,54]. In breast cancer, Annis et al. demonstrated the participation of integrin $\alpha V\beta 3$ in tumor invasion via activation of SRC/MAPK signaling and FRA-1 phosphorylation [55].

Although some reports on GBM suggest an interaction between integrins and uPAR, no concrete evidence in this regard has been published. Among the few reports on this topic are the results published by Veeravalli et al., who demonstrated the downregulation of the expression of several integrins, such as $\alpha 1$, $\alpha 2$, $\alpha 6$, $\alpha 7$, $\alpha 9$, and αV , as well as $\beta 1$ and $\beta 3$, in response to the reduction in uPAR mRNA levels [56]. Their research underscores the critical roles of integrins, uPAR, and MMP9 in glioma tumor biology and proposes a possible interaction model between them [57].

Given that $I\alpha V$ and uPAR are relevant antigens associated with poor clinical prognosis in human GBM, we focused our efforts on understanding these kinds of interactions. By employing two high-grade GBM cell lines that express both proteins, we detected interaction between these proteins, as demonstrated by Co-IP assays and CM. Since no uPAR was detected in the low-grade glioma cell line, we attempted to induce its expression by transfecting the uPAR gene sequence, termed PLAUR. Interestingly, no $I\alpha V$ /uPAR interaction was observed in these cells, suggesting that the mere presence of the protein in low-grade glioma cells is not sufficient to establish a positive interaction. This finding suggested that an additional factor participates in the interaction between these two proteins.

Glycosylation plays a significant role in protein interactions, especially in cell membrane proteins, where a broad spectrum of glycan structures is observed. Aberrant glycosylation refers to the particular glyco-phenotype of cancer cells and involves modification of the glycosylation profile of normal cell progenitors and is concomitant with the multistage process of malignant transformation [36]. The glyco-phenotype of tumor cells may be based primarily on N- or O-glycans, depending on the biology of the tumor. While in neuroblastoma, the glyco-phenotype is mostly expressed based on O-glycans [58], the glycosylation profile found in GBM is primarily expressed by N-glycans [59]. An altered glycosylation profile has been associated with cellular features that promote tumor progression, such as adhesion to the ECM, migration, invasion, inhibition of apoptosis, host immunoregulation and resistance to chemotherapy [60].

The glycosylation of integrins has been demonstrated to be relevant for cell adhesion, migration, and survival in tumor cells [61–63]. There are more than 20 potential N-linked glycosylation sites on $\alpha\beta$ integrin dimers [61]. Additionally, integrin αV specifically has 12 putative N-glycosylation sites. The presence of these N-glycan core structures has been demonstrated to be crucial for several reasons; they are essential for integrin heterodimerization, stabilization of the conformation, expression at the cell membrane, and interaction with ligands [64,65].

The structural association between integrins and uPAR has been extensively reported. Simon et al. [66] and Zhang et al. [67] reported that the surface loop of the β -propeller

domain of the integrin α -chain in $\alpha3\beta1$ and $\alphaM\beta2$ heterodimers functionally associates with uPAR. Subsequently, Chaurasia et al. further showed that integrin $\alpha5\beta1$ interacts with the domain III region of uPAR [68]. Additionally, Ahn et al. suggested that interaction with uPAR requires the expression of the complete $\alpha\beta$ heterodimer (e.g., $\alphaV\beta6$) rather than individual subunits [33]. Additional insights through docking simulations of integrin $\alphaV\beta3$ and uPAR showed that the β -propeller region of αV from $\alphaV\beta3$ interacts with domains II and III of uPAR [69].

Although the integrin/uPAR interaction has been well described, the role of glycans in this process has been scarcely evaluated. To the best of our knowledge, only one report has shown that treating melanoma cells with SW inhibits the interaction of αV or $\alpha3$ with uPAR, suggesting an important role for N-glycosylation in this interaction [34]. Similarly, our results demonstrated that N-glycosylation plays a key role in the integrin αV /uPAR interaction since treatment with both SW and PNGase inhibited this interaction, as demonstrated by Co-IP and CM. Of the 12 reported potential glycosylation sites of I α V, six were found in the GBM cell line LN229 (N74, N554, N615, N704, N874, and N945) and only two were found in the low-grade glioma cell line SW1088 (N74 and N874). Interestingly, the glycan profiles of these cells showed substantial differences. The glycosylation profile of I α V obtained from the GBM cell line exhibited a high proportion of complex and hybrid glycans, with a limited presence of oligomannose-type glycans, except at position N945, which contained 100% oligomannose. In contrast, I α V from low-grade glioma glycosylation was characterized exclusively by oligomannose-type glycans at the two glycosylated positions. As mentioned before, the β -propeller domain of integrin is, according to the literature, involved in the interaction with uPAR, with N74 being the only glycosylation site within this domain. Although position N74 of I α V is glycosylated in both cell lines, the glycan profiles differ significantly; the GBM cell line predominantly contains complex-type glycans, while the low-grade glioma cell line primarily contains oligomannose-type glycans. To identify the participating glycan structures, we treated GBM cell lines A172 and LN229 with NeuA, which strongly affects the I α V/uPAR interaction, indicating the significant involvement of sialic acids, which are found at all glycosylated positions. Moreover, incubation with PHA-L, which binds to $\beta1$ -6 branched N-glycans, also inhibited the I α V/uPAR interaction. Conversely, incubation with ConA, which recognizes oligomannose structures, does not inhibit the I α V/uPAR interaction. Our results suggest that $\beta1$ -6 branched glycans could be present at positions N74, N554, and N874. The first site is located within the β -propeller domain, the second is adjacent to it, and the third is near the transmembrane domain, forming part of the Ig domain 3. Considering the role of the integrin β -propeller domain in contacting uPAR, the glycan at N554 is unlikely to participate in the interaction, and the involvement of N874 is even less expected. Therefore, we speculate that the predicted branched $\beta1$ -6 glycan at N74 plays an important role in this interaction. However, further studies should be conducted to evaluate the participation of glycosite N554. In this sense, the analysis of point mutations in the glycosylation sites would be a remarkable asset to identify with greater certainty which position is involved in the evaluated interaction. Sato et al. carried out a series of experiments that demonstrated the involvement of N-glycosylation sites present in the β -propeller as critical players in the interaction between $\alpha5$ and $\beta1$ by point mutation analysis [70]. More recently, the role of N-glycosylation of the $\beta1$ subunit in AKT signaling has also been demonstrated using this technique [71].

To assess the impact of integrin-related glycosylation on the cellular response, we evaluated the phosphorylation of AKT, a known Integrin/uPAR-derived signal transducer [72,73]. The treatment of GBM cell lines with SW inhibited AKT phosphorylation by more than 50%, indicating that N-glycans are involved in AKT-activating signaling.

Similar results were observed after treatment with NeuA, suggesting that sialic acid is a relevant player in this process. We performed the same experiments in cells transfected with PLAUR, which showed an increase in the phosphorylation of AKT, most likely due to the overexpression of uPAR in both cell lines and its inhibition as a consequence of SW and NeuA treatment.

4. Materials and Methods

4.1. Cell Lines

The human low-grade glioma cell line derived from a diffuse astrocytoma (grade II) SW1088 and the human high-grade glioma cell line (grade IV) A172, obtained from the American Type Culture Collection (ATCC, Manassas, VA, USA), were grown in Roswell Park Memorial Institute (RPMI) 1640 medium (Sigma-Aldrich, Burlington, MA, USA). The human GBM cell line (grade IV) LN229 was grown in Dulbecco's modified Eagle's medium (DMEM) (Sigma-Aldrich, MA, USA). The cell lines were supplemented with 10% fetal bovine serum (FBS) (Sigma-Aldrich, MA, USA) and 80 µg/mL gentamicin (Northia, CABA, Argentina). The cells were maintained at 37 °C in a humidified atmosphere containing 5% CO₂, and routine subculture was performed using trypsin-EDTA solution (Thermo Fisher Scientific, Waltham, MA, USA) following standard procedures. Monthly screening for Mycoplasma contamination was conducted using 4',6-diamino-2-phenylindole (DAPI) staining (Vectorlabs, Newark, CA, USA) and visualization under a fluorescence microscope.

4.2. Glycosylation Inhibition and Removal

The cells were cultured in their respective media and incubated with 100 nM swainsonine (SW) (Sigma-Aldrich, MA, USA), 5 UI/mL peptide-N-glycosidase F (PNGase) (New England Biolabs, Ipswich, MA, USA), or 1 UI/mL neuraminidase A (NeuA) (New England Biolabs, MA, USA) for 24 h. The control cells were treated with an equivalent volume of phosphate-buffered saline (PBS). Treatments do not affect the viability or the uPAR and IαV protein expression of the cells (Table S1).

4.3. Lectin Interference Assay

Cell monolayers cultured without FBS were incubated with 20 µg/mL of the lectins Phytohemagglutinin-L (PHA-L) or Concanavalin A (ConA) (Vector Labs, MA, USA) for 1 h at 37 °C. After this incubation, protein co-immunoprecipitation and immunofluorescence were conducted.

4.4. Plasmid DNA Transfection

For overexpression of the uPAR protein, cells were grown to approximately 90% confluence and transfected with the uPAR plasmid (HG10925; Sino Biological, Wayne, PA, USA) using Lipofectamine 2000 reagent (Invitrogen, Carlsbad, MA, USA), according to the manufacturer's instructions. Immunofluorescence or Western blot (WB) assays were also conducted 48 h post transfection.

4.5. Immunofluorescence

A total of 2×10^5 (for A172) or 5×10^5 (for LN229 or SW1088) cells were seeded on coverslips (JSHD, JS, Yancheng City, China) in 6-well plates. The cells were washed with PBS and fixed for 10 min with 4% formalin in PBS at room temperature. Following fixation, the cells were blocked for 30 min with 1% BSA in PBS. Subsequently, the samples were incubated overnight at 4 °C with primary antibodies against IαV (1:200; Abcam Cat# ab179475, RRID:AB_2716738). After washing with PBS, the cells were incubated with FITC-conjugated secondary antibodies (1:200; Abcam Cat# ab6717, RRID:AB_955238) in

PBS for 1 h at room temperature. After three washes with PBS, the cells were incubated with primary antibodies against uPAR (1:50; (Santa Cruz Biotechnology Cat# sc-376494, RRID:AB_11150125) and Alexa 594-conjugated secondary antibodies (1:200; Thermo Fisher Scientific Cat# A-11005, RRID:AB_2534073), as previously described.

For PHA-L (Vector Labs, MA, USA) binding, 0.5 μg of the lectin was incubated overnight at 4 °C. After washing with PBS, the cells were incubated with 0.5 μg of streptavidin-FITC (Vector Labs, USA) in PBS for 1h at room temperature.

Finally, the coverslips were incubated with 0.1 $\mu\text{g}/\text{mL}$ DAPI (Sigma-Aldrich, MA, USA) for 15 min at room temperature and mounted on glass slides with 80% glycerol in PBS.

4.6. Confocal Microscopy

Confocal microscopy (CM) was performed using an inverted Leica TCS SP8 spectral scanning confocal microscope (Leica Microsystem, Wetzlar, Germany) equipped with specific lasers for the fluorochromes Alexa Fluor-594 (exc: 561 nm), FITC (exc: 488 nm) and DAPI (exc: 405 nm). Observation was conducted with a 60X objective, and the images were captured by sequential scanning configuring different detection channels for each fluorochrome using LasX software (v3.7.4.23463 Leica Microsystem, WZ, Germany) to digitize images with a resolution of 1024 \times 1024 pixels.

Co-localization analysis of proteins was performed using Pearson's correlation coefficient analysis, which was implemented through the Fiji image processing package (RRID:SCR_002285) of ImageJ software (v1.54f; RRID:SCR_003070). Briefly, each pixel in the first image was paired with the corresponding pixel in the second image, creating an intensity values dataset resulting from the combination of both channels. The Pearson's correlation coefficient values were interpreted as follows; a value of +1 indicated a perfect positive correlation, values greater than +0.5 denoted a positive interaction, 0 represented no correlation, and -1 indicated a perfect negative correlation.

4.7. Protein Co-Immunoprecipitation

Protein co-immunoprecipitation (Co-IP) was conducted using the Pierce™ Direct IP Kit (Invitrogen, MA, USA) following the manufacturer's protocol. Briefly, cells at 90% confluence were lysed with lysis buffer containing protease inhibitor cocktail (Sigma-Aldrich, MA, USA) at 4 °C and centrifuged at 13,000 \times g for 10 min. The supernatant was incubated overnight at 4 °C on an orbital shaker with agarose columns containing 5 μg of anti-I α V (Abcam, CB, Cambridge, UK; Cat# ab179475; RRID:AB_2716738) or 4 μg of anti-uPAR (Ab221680, Abcam, CB, United Kingdom) antibodies. The proteins retained in the column were washed and eluted using an elution buffer to obtain the desired fraction. Immunoprecipitated proteins were analyzed by WB.

4.8. SDS-PAGE and Western Blot

Monolayers containing 5 \times 10⁵ cells were lysed with RIPA buffer supplemented with protease and phosphatase inhibitors (Sigma-Aldrich, MA, USA). The protein lysates were clarified, and the protein concentrations were normalized using the Pierce™ BCA Protein Assay Kit (Thermo Fisher Scientific, MA, USA). Immunoprecipitated proteins or 30 μg of total cell lysates were subjected to electrophoresis on polyacrylamide gels, followed by semidry transfer to 0.45 μm polyvinylidene difluoride membranes (GE Healthcare, Chicago, IL, USA). The membranes were blocked with low-fat milk and then incubated overnight at 4 °C with primary antibodies against I α V (1:5000, Abcam Cat# ab179475, RRID:AB_2716738), uPAR (1:100, Santa Cruz Biotechnology Cat# sc-376494, RRID:AB_11150125), AKT (1:500, R and D Systems Cat# AF1775, RRID:AB_354982), phospho-AKT (pAKT) (1:500, PACO02670, Assay Genie, DUB, Dublin, Ireland), and

β -tubulin (1:5000, BD Biosciences Cat# 556321, RRID:AB_396360). After washing, the membranes were incubated for an hour with an HRP-conjugated secondary antibody against rabbit (Bio-Rad Cat# 170-6515, RRID:AB_11125142) or mouse (Bio-Rad Cat# 170-6516, RRID:AB_11125547) immunoglobulins. Finally, the membranes were visualized using a bioluminescence kit (Bio-Lumina, PBL, BsAs, Argentina) and membrane images were captured using a C-DiGit[®] Blot Scanner (LI-COR, Lincoln, NE, USA). The pAKT/AKT variation is expressed as the percentage change in the difference between the optical densities of pAKT and AKT in treated cells, relative to the difference obtained between these bands in untreated cells.

4.9. Protein Concentration

For mass spectrometry assays, immunoprecipitates were concentrated using Vivaspin[®] 500 Centrifugal Concentrators (Sartorius AG, UGOE, Göttingen, Germany), following the manufacturer's instructions. Immunoprecipitation products were centrifuged at $12,000 \times g$ for 2 h until a final volume of 50 μ L was reached. The concentrated samples were subjected to N-glycan analysis by mass spectrometry.

4.10. Mass Spectrometry

Mass spectrometry (MS) was conducted on I α V from cell line cultures. After the electrophoretic run, the gels were fixed for 3 h in a solution containing 50% methanol and 2% phosphoric acid. Following three washes, the gels were incubated for an hour in a balancing solution composed of 33% methanol, 17% ammonium sulfate, and 3% phosphoric acid. Next, Coomassie Brilliant Blue G 250 (Sigma Aldrich, MA, USA) was added at a final concentration of 0.06%, and the gels were incubated overnight. After three additional washes with bidistilled water under agitation, the bands corresponding to the proteins of interest were excised.

Protein digestion and MS analysis were performed at the Proteomics Service of CE-QUIBIEM at the University of Buenos Aires/CONICET. In brief, the excised bands were sequentially washed with 50 mM ammonium bicarbonate (AB), 25 mM AB, 50% acetonitrile (ACN), and 100% ACN. The products were subsequently reduced and alkylated with 10 mM dithiothreitol and 20 mM iodoacetamide. In-gel digestion with 100 ng of trypsin (Promega, Madison, WI, USA) in 25 mM AB was carried out overnight at 37 °C. The resulting peptides were recovered by elution with 50% ACN/0.5% trifluoroacetic acid and concentrated by rapid vacuum drying. Finally, the samples were resuspended in 15 μ L of water containing 0.1% formic acid. The peptide digestion products were analyzed by nanoLC-MS/MS using a nanoHPLC EASY-nLC 1000 (Thermo Fisher Scientific, USA) coupled to a QExactive mass spectrometer. A C18 precolumn (Acclaim PepMap 3 μ m, 100 Å, 75 μ m \times 20 mm) was used for peptide desalination, followed by a 75 min gradient of H₂O:ACN at a flow rate of 33 nL/min with an Easy Spray C18 column (2 mm \times 150 mm). The data-dependent MS² method was used to fragment the most intense peaks of each cycle. The raw MS data were processed using Proteome Discoverer software (RRID:SCR_014477), version 2.1.1.21 (Thermo Fisher Scientific, MA, USA). Fragmentation of a glycopeptide precursor ($[M + 2H]^+$) clearly showed the decomposition of the oligosaccharide portion permitting the assignment of the peptide moiety (m/z) (Table S1). Accordingly, as an example, in the N-glycopeptide ANTTQPGIVEGGQVLK that contains the glycosite N74 detected at 3484.52 ($[M + 2H]^{3+}$) m/z peak could be assigned the glycan HexNAc(3)Hex(6)NeuAc(1). An incomplete precursor of this glycan was found at 3193.43 ($[M + 2H]^{3+}$) m/z peak (highlighted). The glycan structures found were corroborated using the GlyConnect platform, and graphical representations were obtained from the GlyTouCan repository.

4.11. Statistical Analysis

Statistical analysis was performed using Prism 8 software (GraphPad Inc, San Diego, CA, USA, RRID:SCR_002798). The data are presented as the mean values \pm standard deviations. Prior to statistical testing, the normality of the data was assessed. For comparisons involving two independent samples, the Mann–Whitney test was employed. Multiple comparisons between experimental groups were analyzed using ANOVA followed by Tukey's post hoc test. Significance thresholds were set at * $p < 0.05$, ** $p < 0.01$, and *** $p < 0.001$.

5. Conclusions

Our findings demonstrate for the first time the interaction of I α V with uPAR in GBM cells and the major role of N-glycans, suggesting the essential participation of β 1-6 branched N-glycans as well as sialic acids. Both structures are found at glycosylation position N74 of I α V within the β -propeller domain. This work provides novel and valuable insights into the interaction between I α V and uPAR, two significant proteins in GBM tumor biology, highlighting the crucial role of glycosylation.

Supplementary Materials: The following supporting information can be downloaded at: <https://www.mdpi.com/article/10.3390/ijms26115310/s1>.

Author Contributions: Conceptualization, G.M.F. and M.R.G.; methodology, G.M.F., H.A.C., A.C.N., J.O.C., S.R. and C.A.G.; investigation, G.M.F., V.I.S. and M.R.G.; data curation, G.M.F. and M.R.G.; writing—original draft preparation, G.M.F. and M.R.G.; writing—review and editing, H.A.C. and V.I.S.; funding acquisition, V.I.S. and M.R.G. All authors have read and agreed to the published version of the manuscript.

Funding: This work was funded by Universidad Nacional de Quilmes (grant number: EXPTE 2283/22) and the Instituto Nacional del Cáncer, Argentina (grant number: EXPTE 827-492/23).

Institutional Review Board Statement: Not applicable.

Informed Consent Statement: Not applicable.

Data Availability Statement: Data are contained within the article and Supplementary Materials.

Acknowledgments: G.M.F., A.C.N., J.O.C. and S.R. are research fellows of CONICET.

Conflicts of Interest: The authors declare that they have no competing interests.

Abbreviations

The following abbreviations are used in this manuscript:

AB	Ammonium bicarbonate
ACN	Acetonitrile
CM	Confocal microscopy
Co-IP	Co-Immunoprecipitation
ConA	Concanavalin A
DAPI	4',6-diamidino-2-phenylindole
DMEM	Dulbecco's Modified Eagle's Medium
ECM	Extracellular Matrix
FAK	Focal adhesion kinase
FBS	Fetal bovine serum
GBM	Glioblastoma
I α V	Integrin Av
MAPK	Mitogen-activated protein kinase
MS	Mass spectrometry
NeuA	Neuraminidase A

NeuAc	N-Acetylneuraminic acid
NeuGc	N-Glycolylneuraminic acid
pAKT	Phospho-AKT
PBS	Phosphate-buffered saline
PHA-L	Phytohemagglutinin-L
PNGase	Peptide-N-Glycosidase F
RPMI	Roswell Park Memorial Institute
SW	Swainsonine
uPA	Urokinase-type plasminogen activator
uPAR	Urokinase-type plasminogen activator receptor
WB	Western blot

References

1. Mallick, S.; Benson, R.; Hakim, A.; Rath, G.K. Management of glioblastoma after recurrence: A changing paradigm. *J. Egypt. Natl. Cancer Inst.* **2016**, *28*, 199–210. [[CrossRef](#)] [[PubMed](#)]
2. Barczyk, M.; Carracedo, S.; Gullberg, D. Integrins. *Cell Tissue Res.* **2010**, *339*, 269–280. [[CrossRef](#)] [[PubMed](#)]
3. Campbell, I.D.; Humphries, M.J. Integrin structure, activation, and interactions. *Cold Spring Harb. Perspect. Biol.* **2011**, *3*, a004994. [[CrossRef](#)]
4. Peng, Z.; Hao, M.; Tong, H.; Yang, H.; Huang, B.; Zhang, Z.; Luo, K.Q. The interactions between integrin $\alpha_5\beta_1$ of liver cancer cells and fibronectin of fibroblasts promote tumor growth and angiogenesis. *Int. J. Biol. Sci.* **2022**, *18*, 5019–5037. [[CrossRef](#)]
5. Zhang, Y.; Reif, G.; Wallace, D.P. Extracellular matrix, integrins, and focal adhesion signaling in polycystic kidney disease. *Cell. Signal.* **2020**, *72*, 109646. [[CrossRef](#)]
6. Wu, D.; Xu, Y.; Ding, T.; Zu, Y.; Yang, C.; Yu, L. Pairing of integrins with ECM proteins determines migrasome formation. *Cell Res.* **2017**, *27*, 1397–1400. [[CrossRef](#)]
7. Lainé, A.; Labiad, O.; Hernandez-Vargas, H.; This, S.; Sanlaville, A.; Léon, S.; Dalle, S.; Sheppard, D.; Travis, M.A.; Paidassi, H.; et al. Regulatory T cells promote cancer immune-escape through integrin $\alpha v\beta 8$ -mediated TGF- β activation. *Nat. Commun.* **2021**, *12*, 6228. [[CrossRef](#)]
8. Kumari, S.; Kumar, P. Identification and characterization of putative biomarkers and therapeutic axis in Glioblastoma multiforme microenvironment. *Front. Cell Dev. Biol.* **2023**, *11*, 1236271. [[CrossRef](#)]
9. Suresh, A.; Biswas, A.; Perumal, S.; Khurana, S. Periostin and Integrin Signaling in Stem Cell Regulation. *Adv. Exp. Med. Biol.* **2019**, *1132*, 163–176. [[CrossRef](#)]
10. Ellis, S.J.; Tanentzapf, G. Integrin-mediated adhesion and stem-cell-niche interactions. *Cell Tissue Res.* **2010**, *339*, 121–130. [[CrossRef](#)]
11. Hoshino, A.; Costa-Silva, B.; Shen, T.-L.; Rodrigues, G.; Hashimoto, A.; Mark, M.T.; Molina, H.; Kohsaka, S.; Di Giannatale, A.; Ceder, S.; et al. Tumour exosome integrins determine organotropic metastasis. *Nature* **2015**, *527*, 329–335. [[CrossRef](#)] [[PubMed](#)]
12. Zhang, L.; Shan, X.; Meng, X.; Gu, T.; Guo, L.; An, X.; Jiang, Q.; Ge, H.; Ning, X. Novel Integrin $\alpha v\beta 3$ -specific ligand for the sensitive diagnosis of glioblastoma. *Mol. Pharm.* **2019**, *16*, 3977–3984. [[CrossRef](#)]
13. Nakada, M.; Nambu, E.; Furuyama, N.; Yoshida, Y.; Takino, T.; Hayashi, Y.; Sato, H.; Sai, Y.; Tsuji, T.; Miyamoto, K.-I.; et al. Integrin $\alpha 3$ is overexpressed in glioma stem-like cells and promotes invasion. *Br. J. Cancer* **2013**, *108*, 2516–2524. [[CrossRef](#)]
14. Delamarre, E.; Taboubi, S.; Mathieu, S.; Bérenguer, C.; Rigot, V.; Lissitzky, J.-C.; Figarella-Branger, D.; Ouafik, L.; Luis, J. Expression of Integrin $\alpha 6\beta 1$ Enhances Tumorigenesis in Glioma Cells. *Am. J. Pathol.* **2009**, *175*, 844–855. [[CrossRef](#)]
15. Bello, L.; Francolini, M.; Marthyn, P.; Zhang, J.; Carroll, R.S.; Nikas, D.C.; Strasser, J.F.; Villani, R.; Cheresch, D.A.; Black, P.M. $\alpha v\beta 3$ and $\alpha v\beta 5$ Integrin Expression in Glioma Periphery. *Neurosurgery* **2001**, *49*, 380–390. [[CrossRef](#)]
16. Gladson, C.L. Expression of integrin alpha v beta 3 in small blood vessels of glioblastoma tumors. *J. Neuropathol. Exp. Neurol.* **1996**, *55*, 1143–1149. [[CrossRef](#)]
17. Schittenhelm, J.; Schwab, E.I.; Sperveslage, J.; Tatagiba, M.; Meyermann, R.; Fend, F.; Goodman, S.L.; Sipos, B. Longitudinal expression analysis of αv integrins in human gliomas reveals upregulation of integrin $\alpha v\beta 3$ as a negative prognostic factor. *J. Neuropathol. Exp. Neurol.* **2013**, *72*, 194–210. [[CrossRef](#)]
18. Gingras, M.-C.; Roussel, E.; Bruner, J.M.; Branch, C.D.; Moser, R.P. Comparison of cell adhesion molecule expression between glioblastoma multiforme and autologous normal brain tissue. *J. Neuroimmunol.* **1995**, *57*, 143–153. [[CrossRef](#)]
19. Loriger, M.; Krueger, J.S.; O'Neal, M.; Staffin, K.; Felding-Habermann, B. Activation of tumor cell integrin $\alpha v\beta 3$ controls angiogenesis and metastatic growth in the brain. *Proc. Natl. Acad. Sci. USA* **2009**, *106*, 10666–10671. [[CrossRef](#)]
20. Martin, S.; Janouskova, H.; Dontenwill, M. Integrins and p53 pathways in glioblastoma resistance to temozolomide. *Front. Oncol.* **2012**, *2*, 157. [[CrossRef](#)]

21. Stanzani, E.; Pedrosa, L.; Bourmeau, G.; Anezo, O.; Noguera-Castells, A.; Esteve-Codina, A.; Passoni, L.; Matteoli, M.; de la Iglesia, N.; Seano, G.; et al. Dual role of integrin alpha-6 in glioblastoma: Supporting stemness in proneural stem-like cells while inducing radioresistance in mesenchymal stem-like cells. *Cancers* **2021**, *13*, 3055. [[CrossRef](#)] [[PubMed](#)]
22. Casey, J.R.; Petranka, J.G.; Kottra, J.; Fleenor, D.E.; Rosse, W.F. The structure of the urokinase-type plasminogen activator receptor gene. *Blood* **1994**, *84*, 1151–1156. [[CrossRef](#)] [[PubMed](#)]
23. Ghiso, J.A.A. Inhibition of FAK signaling activated by urokinase receptor induces dormancy in human carcinoma cells in vivo. *Oncogene* **2002**, *21*, 2513–2524. [[CrossRef](#)]
24. Vial, E.; Sahai, E.; Marshall, C.J. ERK-MAPK signaling coordinately regulates activity of Rac1 and RhoA for tumor cell motility. *Cancer Cell* **2003**, *4*, 67–79. [[CrossRef](#)]
25. Liu, D.; Ghiso, J.A.; Estrada, Y.; Ossowski, L. EGFR is a transducer of the urokinase receptor initiated signal that is required for in vivo growth of a human carcinoma. *Cancer Cell* **2002**, *1*, 445–457. [[CrossRef](#)]
26. Kjølner, L.; Hall, A. Rac mediates cytoskeletal rearrangements and increased cell motility induced by urokinase-type plasminogen activator receptor binding to vitronectin. *J. Cell Biol.* **2001**, *152*, 1145–1158. [[CrossRef](#)]
27. de Bock, C.E.; Wang, Y. Clinical significance of urokinase-type plasminogen activator receptor (uPAR) expression in cancer. *Med. Res. Rev.* **2004**, *24*, 13–39. [[CrossRef](#)]
28. Persson, M.; Nedergaard, M.K.; Brandt-Larsen, M.; Skovgaard, D.; Jørgensen, J.T.; Michaelsen, S.R.; Madsen, J.; Lassen, U.; Poulsen, H.S.; Kjaer, A. Urokinase-Type Plasminogen Activator Receptor as a Potential PET Biomarker in Glioblastoma. *J. Nucl. Med.* **2016**, *57*, 272–278. [[CrossRef](#)]
29. Gilder, A.S.; Natali, L.; Van Dyk, D.M.; Zalfa, C.; Banki, M.A.; Pizzo, D.P.; Wang, H.; Klemke, R.L.; Mantuano, E.; Gonias, S.L. The Urokinase Receptor Induces a Mesenchymal Gene Expression Signature in Glioblastoma Cells and Promotes Tumor Cell Survival in Neurospheres. *Sci. Rep.* **2018**, *8*, 2982. [[CrossRef](#)]
30. Smith, H.W.; Marshall, C.J. Regulation of cell signalling by uPAR. *Nat. Rev. Mol. Cell Biol.* **2010**, *11*, 23–36. [[CrossRef](#)]
31. Wei, Y.; Lukashev, M.; Simon, D.I.; Bodary, S.C.; Rosenberg, S.; Doyle, M.V.; Chapman, H.A. Regulation of Integrin Function by the Urokinase Receptor. *Science* **1996**, *273*, 1551–1555. [[CrossRef](#)] [[PubMed](#)]
32. Sowmya, G.; Khan, J.M.; Anand, S.; Ahn, S.B.; Baker, M.S.; Ranganathan, S. A site for direct integrin $\alpha v \beta 6$ -uPAR interaction from structural modelling and docking. *J. Struct. Biol.* **2014**, *185*, 327–335. [[CrossRef](#)] [[PubMed](#)]
33. Ahn, S.B.; Mohamedali, A.; Anand, S.; Cheruku, H.R.; Birch, D.; Sowmya, G.; Cantor, D.; Ranganathan, S.; Inglis, D.W.; Frank, R.; et al. Characterization of the interaction between heterodimeric $\alpha v \beta 6$ integrin and urokinase plasminogen activator receptor (uPAR) using functional proteomics. *J. Proteome Res.* **2014**, *13*, 5956–5964. [[CrossRef](#)]
34. Janik, M.E.; Przybyło, M.; Pocheć, E.; Pokrywka, M.; Lityńska, A. Effect of alpha3beta1 and alphavbeta3 integrin glycosylation on interaction of melanoma cells with vitronectin. *Acta Biochim. Pol.* **2010**, *57*, 55–61. [[CrossRef](#)]
35. Munkley, J.; Elliott, D.J. Hallmarks of glycosylation in cancer. *Oncotarget* **2016**, *7*, 35478–35489. [[CrossRef](#)]
36. Hakomori, S. Tumor malignancy defined by aberrant glycosylation and sphingo(glyco)lipid metabolism. *Cancer Res.* **1996**, *56*, 5309–5318.
37. Kannagi, R.; Yin, J.; Miyazaki, K.; Izawa, M. Current relevance of incomplete synthesis and neo-synthesis for cancer-associated alteration of carbohydrate determinants—Hakomori’s concepts revisited. *Biochim. Biophys. Acta* **2008**, *1780*, 525–531. [[CrossRef](#)]
38. Lehmann, M.; El Battari, A.; Abadie, B.; Martin, J.M.; Marvaldi, J. Role of alpha v beta 5 and alpha v beta 6 integrin glycosylation in the adhesion of a colonic adenocarcinoma cell line (HT29-D4). *J. Cell. Biochem.* **1996**, *61*, 266–277. [[CrossRef](#)]
39. Pocheć, E.; Bubka, M.; Rydlewska, M.; Janik, M.; Pokrywka, M.; Lityńska, A. Aberrant glycosylation of $\alpha v \beta 3$ integrin is associated with melanoma progression. *Anticancer Res.* **2015**, *35*, 2093–2103.
40. Behrendt, N.; Rønne, E.; Ploug, M.; Petri, T.; Løber, D.; Nielsen, L.S.; Schleuning, W.D.; Blasi, F.; Appella, E.; Danø, K. The human receptor for urokinase plasminogen activator. NH2-terminal amino acid sequence and glycosylation variants. *J. Biol. Chem.* **1990**, *265*, 6453–6460. [[CrossRef](#)]
41. Kjaergaard, M.; Hansen, L.V.; Jacobsen, B.; Gardsvoll, H.; Ploug, M. Structure and ligand interactions of the urokinase receptor (uPAR). *Front. Biosci.* **2008**, *13*, 5441–5461. [[CrossRef](#)] [[PubMed](#)]
42. Mukherjee, M.M.; Bond, M.R.; Abramowitz, L.K.; Biesbrock, D.; Woodroffe, C.C.; Kim, E.J.; Swenson, R.E.; Hanover, J.A. Tools and tactics to define specificity of metabolic chemical reporters. *Front. Mol. Biosci.* **2023**, *10*, 1286690. [[CrossRef](#)]
43. Mukherjee, M.M.; Biesbrock, D.; Abramowitz, L.K.; Pavan, M.; Kumar, B.; Walter, P.J.; Azadi, P.; Jacobson, K.A.; Hanover, J.A. Selective bioorthogonal probe for N-glycan hybrid structures. *Nat. Chem. Biol.* **2025**, *21*, 681–692. [[CrossRef](#)]
44. Elbein, A.D. Inhibitors of the biosynthesis and processing of N-linked oligosaccharide chains. *Annu. Rev. Biochem.* **1987**, *56*, 497–534. [[CrossRef](#)]
45. Maley, F.; Trimble, R.B.; Tarentino, A.L.; Plummer, T.H., Jr. Characterization of glycoproteins and their associated oligosaccharides through the use of endoglycosidases. *Anal. Biochem.* **1989**, *180*, 195–204. [[CrossRef](#)]
46. Gabri, M.R.; Otero, L.L.; Gomez, D.E.; Alonso, D.F. Exogenous incorporation of neuge-rich mucin augments n-glycolyl sialic acid content and promotes malignant phenotype in mouse tumor cell lines. *J. Exp. Clin. Cancer Res.* **2009**, *28*, 146. [[CrossRef](#)]

47. Dhar, C.; Sasmal, A.; Varki, A. From “Serum Sickness” to “Xenosialitis”: Past, Present, and Future Significance of the Non-human Sialic Acid Neu5Gc. *Front. Immunol.* **2019**, *10*, 807. [[CrossRef](#)]
48. Blasi, F. uPA, uPAR, PAI-I: Key intersection of proteolytic, adhesive and chemotactic highways? *Immunol. Today* **1997**, *18*, 415–417. [[CrossRef](#)]
49. Sidenius, N.; Blasi, F. The urokinase plasminogen activator system in cancer: Recent advances and implication for prognosis and therapy. *Cancer Metastasis Rev.* **2003**, *22*, 205–222. [[CrossRef](#)]
50. Desgrosellier, J.S.; Cheresh, D.A. Integrins in cancer: Biological implications and therapeutic opportunities. *Nat. Rev. Cancer* **2010**, *10*, 9–22. [[CrossRef](#)]
51. Hamidi, H.; Ivaska, J. Every step of the way: Integrins in cancer progression and metastasis. *Nat. Rev. Cancer* **2018**, *18*, 533–548. [[CrossRef](#)] [[PubMed](#)]
52. Cáceres-Calle, D.; Torre-Cea, I.; Marcos-Zazo, L.; Carrera-Aguado, I.; Guerra-Paes, E.; Berlana-Galán, P.; Muñoz-Félix, J.M.; Sánchez-Juanes, F. Integrins as Key Mediators of Metastasis. *Int. J. Mol. Sci.* **2025**, *26*, 904. [[CrossRef](#)] [[PubMed](#)]
53. Gao, H.; Peng, C.; Liang, B.; Shahbaz, M.; Liu, S.; Wang, B.; Sun, Q.; Niu, Z.; Niu, W.; Liu, E.; et al. $\beta 6$ integrin induces the expression of metalloproteinase-3 and metalloproteinase-9 in colon cancer cells via ERK-ETS1 pathway. *Cancer Lett.* **2014**, *354*, 427–437. [[CrossRef](#)]
54. Cantor, D.I.; Cheruku, H.R.; Nice, E.C.; Baker, M.S. Integrin $\alpha\beta 6$ sets the stage for colorectal cancer metastasis. *Cancer Metastasis Rev.* **2015**, *34*, 715–734. [[CrossRef](#)]
55. Annis, M.G.; Ouellet, V.; Rennhack, J.P.; L’esperance, S.; Rancourt, C.; Mes-Masson, A.-M.; Andrechek, E.R.; Siegel, P.M. Integrin-uPAR signaling leads to FRA-1 phosphorylation and enhanced breast cancer invasion. *Breast Cancer Res.* **2018**, *20*, 9. [[CrossRef](#)]
56. Veeravalli, K.K.; Chetty, C.; Ponnala, S.; Gondi, C.S.; Lakka, S.S.; Fassett, D.; Klopfenstein, J.D.; Dinh, D.H.; Gujrati, M.; Rao, J.S. MMP-9, uPAR and cathepsin B silencing downregulate integrins in human glioma xenograft cells in vitro and in vivo in nude mice. *PLoS ONE* **2010**, *5*, e11583. [[CrossRef](#)]
57. Veeravalli, K.K.; Rao, J.S. MMP-9 and uPAR regulated glioma cell migration. *Cell Adhes. Migr.* **2012**, *6*, 509–512. [[CrossRef](#)]
58. Cuello, H.A.; Segatori, V.I.; Albertó, M.; Gulino, C.A.; Aschero, R.; Camarero, S.; Mutti, L.G.; Madauss, K.; Alonso, D.F.; Lubieniecki, F.; et al. Aberrant O-glycosylation modulates aggressiveness in neuroblastoma. *Oncotarget* **2018**, *9*, 34176–34188. [[CrossRef](#)]
59. Cuello, H.A.; Ferreira, G.M.; Gulino, C.A.; Toledo, A.G.; Segatori, V.I.; Gabri, M.R. Terminally sialylated and fucosylated complex N-glycans are involved in the malignant behavior of high-grade glioma. *Oncotarget* **2020**, *11*, 4822–4835. [[CrossRef](#)]
60. Pinho, S.S.; Reis, C.A. Glycosylation in cancer: Mechanisms and clinical implications. *Nat. Rev. Cancer* **2015**, *15*, 540–555. [[CrossRef](#)]
61. Gu, J.; Taniguchi, N. Regulation of integrin functions by N-glycans. *Glycoconj. J.* **2004**, *21*, 9–15. [[CrossRef](#)] [[PubMed](#)]
62. Gu, J.; Isaji, T.; Sato, Y.; Kariya, Y.; Fukuda, T. Importance of N-Glycosylation on $\alpha 5\beta 1$ Integrin for Its Biological Functions. *Biol. Pharm. Bull.* **2009**, *32*, 780–785. [[CrossRef](#)] [[PubMed](#)]
63. Janik, M.E.; Lityńska, A.; Vereecken, P. Cell migration—The role of integrin glycosylation. *Biochim. Biophys. Acta* **2010**, *1800*, 545–555. [[CrossRef](#)]
64. Hang, Q.; Isaji, T.; Hou, S.; Wang, Y.; Fukuda, T.; Gu, J. A Key Regulator of Cell Adhesion: Identification and Characterization of Important N-Glycosylation Sites on Integrin $\alpha 5$ for Cell Migration. *Mol. Cell. Biol.* **2017**, *37*, e00558-16. [[CrossRef](#)]
65. Cai, X.; Thinn, A.M.M.; Wang, Z.; Shan, H.; Zhu, J. The importance of N-glycosylation on $\beta 3$ integrin ligand binding and conformational regulation. *Sci. Rep.* **2017**, *7*, 4656. [[CrossRef](#)]
66. Simon, D.I.; Wei, Y.; Zhang, L.; Rao, N.K.; Xu, H.; Chen, Z.; Liu, Q.; Rosenberg, S.; Chapman, H.A. Identification of a Urokinase Receptor-Integrin Interaction Site. *J. Biol. Chem.* **2000**, *275*, 10228–10234. [[CrossRef](#)]
67. Zhang, F.; Tom, C.C.; Kugler, M.C.; Ching, T.-T.; Kreidberg, J.A.; Wei, Y.; Chapman, H.A. Distinct ligand binding sites in integrin $\alpha 3\beta 1$ regulate matrix adhesion and cell–cell contact. *J. Cell Biol.* **2003**, *163*, 177–188. [[CrossRef](#)]
68. Chaurasia, P.; Aguirre-Ghiso, J.A.; Liang, O.D.; Gardsvoll, H.; Ploug, M.; Ossowski, L. A region in urokinase plasminogen receptor domain III controlling a functional association with $\alpha 5\beta 1$ integrin and tumor growth. *J. Biol. Chem.* **2006**, *281*, 14852–14863. [[CrossRef](#)]
69. Degryse, B.; Resnati, M.; Czekay, R.-P.; Loskutoff, D.J.; Blasi, F. Domain 2 of the urokinase receptor contains an integrin-interacting epitope with intrinsic signaling activity: Generation of a new integrin inhibitor. *J. Biol. Chem.* **2005**, *280*, 24792–24803. [[CrossRef](#)]
70. Sato, Y.; Isaji, T.; Tajiri, M.; Yoshida-Yamamoto, S.; Yoshinaka, T.; Somehara, T.; Fukuda, T.; Wada, Y.; Gu, J. An N-glycosylation site on the beta-propeller domain of the integrin $\alpha 5$ subunit plays key roles in both its function and site-specific modification by beta1,4-N-acetylglucosaminyltransferase III. *J. Biol. Chem.* **2009**, *284*, 11873–11881. [[CrossRef](#)]
71. Cao, L.; Wu, Y.; Wang, X.; Li, X.; Tan, Z.; Guan, F. Role of Site-Specific Glycosylation in the I-Like Domain of Integrin $\beta 1$ in Small Extracellular Vesicle-Mediated Malignant Behavior and FAK Activation. *Int. J. Mol. Sci.* **2021**, *22*, 1770. [[CrossRef](#)] [[PubMed](#)]

72. Yu, Q.; Xiao, W.; Sun, S.; Sohrabi, A.; Liang, J.; Seidlits, S.K. Extracellular Matrix Proteins Confer Cell Adhesion-Mediated Drug Resistance Through Integrin αv in Glioblastoma Cells. *Front. Cell Dev. Biol.* **2021**, *9*, 616580. [[CrossRef](#)] [[PubMed](#)]
73. Tang, C.-H.; Hill, M.L.; Brumwell, A.N.; Chapman, H.A.; Wei, Y. Signaling through urokinase and urokinase receptor in lung cancer cells requires interactions with $\beta 1$ integrins. *J. Cell Sci.* **2008**, *121*, 3747–3756. [[CrossRef](#)]

Disclaimer/Publisher’s Note: The statements, opinions and data contained in all publications are solely those of the individual author(s) and contributor(s) and not of MDPI and/or the editor(s). MDPI and/or the editor(s) disclaim responsibility for any injury to people or property resulting from any ideas, methods, instructions or products referred to in the content.